The EMBO Journal vol.14 no.1 pp.76–87, 1995

Functional interaction of Nic96p with a core nucleoporin complex consisting of Nsp1p, Nup49p and a novel protein Nup57p

Paola Grandi, Nick Schlaich, Hildegard Tekotte and Eduard C.Hurt[1]

EMBL, Meyerhofstrasse 1, Postfach 1022.09, D-69117 Heidelberg, Germany

[1]Corresponding author

Communicated by E.C.Hurt

Nic96p has been isolated previously in a complex together with the nuclear pore proteins Nsp1p, Nup49p and a p54 polypeptide. In a genetic screen for Nsp1p-interacting components, we now find *NIC96*, as well as a novel gene *NUP57* which encodes the p54 protein (called Nup57p). Nup57p which is essential for cell growth contains GLFG repeats in the N-terminal half and heptad repeats in the C-terminal half. The domain organization of Nic96p is more complex: N-terminally located heptad repeats mediate binding to a trimeric Nsp1p–Nup49p–Nup57p complex, but are not required for the formation of this core complex; single amino acid substitutions in the central domain yield thermosensitive mutants, which do not impair interaction with the Nsp1 complex; the C-terminal domain is neither essential nor required for binding to the nucleoporin complex, but strikingly mutations in this part cause synthetic lethality with *nsp1* and *nup57* mutant alleles. Since a strain in which the Nic96p heptad repeats were deleted shows, similar to *nsp1* and *nup49* mutants, cytoplasmic mislocalization of a nuclear reporter protein, we propose that the interaction of the heterotrimeric Nsp1p–Nup49p–Nup57p core complex with Nic96p is required for protein transport into the nucleus.

Key words: heptad repeat/nuclear envelope/nuclear pore complex/nucleocytoplasmic transport/yeast

Introduction

Nuclear pore complexes (NPCs) form proteinaceous channels in the nuclear membrane of eukaryotic cells that allow transport of molecules between the nuclear and the cytoplasmic compartments (for reviews see Akey, 1992; Forbes, 1992; Fabre and Hurt, 1994; Panté and Aebi, 1994). The architecture of the NPC has been studied extensively by electron microscopy (EM) and reconstructed in 3-D maps by computer-aided analysis of amphibian oocyte nuclear envelopes (NE) particularly rich in NPCs (Unwin and Milligan, 1982; Akey, 1989; Jarnik and Aebi, 1991; Hinshaw *et al.*, 1992; Akey and Radermacher, 1993). Accordingly, the NPC is formed by an octagonal spoke assembly sandwiched between a cytoplasmic ring and a nucleoplasmic ring, which themselves comprise eight morphologically similar subunits. In the central channel embraced by the spokes sits the 'plug' or 'transporter' (Unwin and Milligan, 1982; Akey, 1990; Reichelt *et al.*, 1990; Akey and Radermacher, 1993). Filaments and globular particles are attached to the cytoplasmic ring and a cage-like filamentous assembly (called the nuclear fishtrap or basket) protrudes from the nucleoplasmic ring into the nucleus (Ris, 1989; Jarnik and Aebi, 1991; Goldberg and Allen, 1992).

Nuclear pores are open for diffusion of small molecules (up to 40–60 kDa; Bonner, 1975; Feldherr *et al.*, 1984) probably through small channels located between the eight spokes (Hinshaw *et al.*, 1992) or, alternatively, between the spokes and the central 'plug' (Akey and Radermacher, 1993). The signal-, energy- and temperature-dependent transport of larger substrates [proteins and ribonucleoproteins (RNPs)], however, should occur through the central channel occupied by the 'transporter' (Akey, 1990; Akey and Radermacher, 1993). The filaments on the cytoplasmic side and the cage-like structure on the nucleoplasmic side of the NPC may be involved in docking and delivery of the transport substrate to the NPC (Feldherr *et al.*, 1984; Richardson *et al.*, 1988; Panté and Aebi, 1993).

The molecular composition of the NPC, although far from being complete, counts up to now for about a dozen different nuclear pore proteins (for recent reviews see Forbes, 1992; Fabre and Hurt, 1994). Nucleoporins were identified with the help of antibodies generated against NE-enriched fractions of isolated nuclei (Dwyer and Blobel, 1976; Snow *et al.*, 1987; Dabauvalle *et al.*, 1988; Featherstone *et al.*, 1988; Hurt, 1988; Davis and Fink, 1990; Wente *et al.*, 1992) and by genetic approaches in yeast (Wimmer *et al.*, 1992; Belanger *et al.*, 1994; Doye *et al.*, 1994; Fabre *et al.*, 1994). Recently, a biochemical procedure to obtain highly purified yeast NPCs on a large scale was developed which allows isolation of the numerous nuclear pore proteins (Rout and Blobel, 1993).

The primary amino acid sequence of a large number of nucleoporins is characterized by evolutionarily conserved short amino acid repeats ('FSFG' and 'GLFG' type) whose function is still unknown (Nehrbass *et al.*, 1990; Loeb *et al.*, 1993); on the other hand, motifs or domains with a predictable secondary structure were detected in some nuclear pore proteins, e.g. membrane-spanning sequences in the integral membrane proteins rat gp210 (Gerace *et al.*, 1982; Wozniak *et al.*, 1989; Greber *et al.*, 1990; Wozniak and Blobel, 1992), rat POM121 (Hallberg *et al.*, 1993) and yeast Pom152p (Wozniak *et al.*, 1994), and nucleic acid binding domains in rat NUP153 (Sukegawa and Blobel, 1993) and yeast Nup145p, Nup116p and Nup100p (Fabre *et al.*, 1994).

Although immuno-EM analysis allowed the localization some of the nuclear pore proteins on distinct substructures of the NPC (Cordes *et al.*, 1991, 1993; Panté and Aebi, 1993; Wilken *et al.*, 1993; Panté *et al.*, 1994), very little

is known about how and where the different nuclear pore proteins assemble to form the 125 MDa structure of the NPC (Reichelt *et al.*, 1990). One might assume that subsets of nuclear pore proteins which perform a common function would first form distinct subcomplexes before assembly into the NPC. An example for the existence of such subcomplexes is the p62 complex isolated from rat liver nuclei (Finlay *et al.*, 1991; Kita *et al.*, 1993). This complex is composed of three subunits (p62, p58 and p54). Similarly, the amphibian homologue of rat p62 was found in a 250 kDa complex isolated from *Xenopus* oocyte NEs (Dabauvalle *et al.*, 1990). Recently, a heterodimeric complex between the glycoprotein p250 and p75 in rat and *Xenopus* was identified (Panté *et al.*, 1994). In yeast, an Nsp1 complex was purified which comprises four proteins Nic96p, Nsp1p, Nup49p and p54 (Grandi *et al.*, 1993). Peptide sequences were obtained from the Nic96 protein which allowed the cloning of the *NIC96* gene (Grandi *et al.*, 1993). As deduced from its amino acid sequence, Nic96p does not contain the typical nucleoporin FSFG/GLFG repeat sequences found in the other members of the complex (Grandi *et al.*, 1993). However, a common structural determinant in Nsp1p, Nup49p and Nic96p is the presence of heptad repeats, shown be involved in the coiled-coil interactions of many other proteins (Steinert and Roop, 1988; Lupas *et al.*, 1991). Similarly, the C-terminal domain of p62, which is homologous to Nsp1p (Carmo-Fonseca *et al.*, 1991), shows heptad repeat organization, and *in vitro* studies using bacterially expressed p62 in fact revealed rod-shaped dimers whose length and periodicity are consistent with an α-helical coiled-coil structure (Buss *et al.*, 1994).

The p62 and the Nsp1 complexes may also have similar functional roles. *In vitro* studies demonstrated that immunodepletion of the p62 complex inhibits the active nuclear uptake of proteins, while the requirement of the p62 complex for NPC formation is still controversial (Dabauvalle *et al.*, 1990; Finlay and Forbes, 1990; Finlay *et al.*, 1991). Similarly, thermosensitive (ts) mutations in the C-terminal domain of Nsp1p cause the cytoplasmic accumulation of nuclear reporter proteins at the restrictive temperature (Nehrbass *et al.*, 1993). Moreover, transcriptional repression of the *NSP1* gene affects nuclear pore biogenesis (Mutvei *et al.*, 1992).

Since relatively little is known about the interactions among nucleoporins which form distinct subcomplexes at the NPC, it would be useful to determine their biogenesis and assembly. Therefore we exploited the versatility of the yeast system by analysing the physico-functional relationships of members of the Nsp1 complex *in vivo*. In this study we present the cloning and characterization of a novel nucleoporin Nup57p, and the results of the molecular and genetic interactions between Nic96p and the other components of the Nsp1 complex.

Results

An extended screen for synthetic lethal mutants of NSP1 reveals many complementation groups including NIC96 and NUP57

Since Nsp1p forms a complex with Nup49p, p54 and Nic96p (Grandi *et al.*, 1993), we also expected to find genetic interactions between the corresponding components. In our previous search for synthetic lethal (sl) mutants of ts *nsp1*, most of the isolated mutants fell into two complementation groups represented by the GLFG nucleoporins Nup116p and Nup49p (Wimmer *et al.*, 1992), but Nic96p and p54 were not among them. The screen, however, was not saturated, because rare complementation groups represented by only one mutant were found. This prompted us to repeat the screen. However, to avoid re-isolation of Nup116p and Nup49p among the mutants, the screening strain RW24 (Wimmer *et al.*, 1992) was transformed with a plasmid containing the *NUP116* and *NUP49* genes before UV mutagenesis and isolation of synthetic lethal mutants (see also Materials and methods). Among the 120 000 screened colonies, 14 new sl mutants were obtained which, as expected, were not complemented by *NUP116* and *NUP49*. Preliminary data indicate that the sl mutants isolated so far belong to at least 11 different complementation groups (H.Tekotte, unpublished results). This suggests the presence of an extended network of genetic interactions involving the nuclear pore protein Nsp1p.

The newly isolated sl mutants were transformed with the cloned *NIC96* gene; two of these mutants, sl57 and sl316, showed red/white colony sectoring and could grow on 5-FOA-containing plates, indicating that they were complemented by the *NIC96* gene (data not shown). By transforming another sl mutant of the new collection, sl29, with a wild-type yeast genomic library (see Materials and methods), a complementing plasmid containing the *NUP57* gene was isolated. This gene encodes Nup57p, a novel protein consisting of 541 amino acids with a predicted molecular weight of 57 kDa (Figure 1A). The primary sequence of Nup57p reveals a two-domain organization: (i) an N-terminal region (residues 1–280) containing three degenerate FXFG (X = S/G) and nine GLFG repeat sequences and (ii) a basic C-terminal region (residues 281–541, isoelectric point = 10.16) predicted to form coiled-coil secondary structures due to the presence of heptad repeats (Figure 1A and B). Sequence comparison of Nup57p with the EMBL data library showed a significant homology of the N-terminal domain to the GLFG-containing domains of Nup145, Nup116p, Nup100p and Nup49p, but no further homologies with other sequenced proteins.

Nup57p is the second GLFG nucleoporin in the purified Nsp1p complex

To analyse the *in vivo* role of Nup57p and its interaction with other NPC components, one *NUP57* gene copy was completely evicted in a diploid strain by homologous recombination with a *nup57::HIS3* null allele in which the *HIS3* gene replaced almost the entire coding sequence of *NUP57* (see Materials and methods). Sporulated heterozygous diploids revealed a 2:2 segregation for viability and the growing progeny were never HIS^+ (data not shown). A 4:0 growing haploid progeny was restored when *nup57::HIS3/NUP57* diploid cells were transformed with an ARS/CEN plasmid containing the wild-type *NUP57* gene prior to tetrad analysis (data not shown). Thus, *NUP57* performs an essential function for cell viability in yeast. Another *NUP57* gene disruption was constructed which fortuitously allowed the expression of a truncated Nup57p C-terminal domain (see Materials and

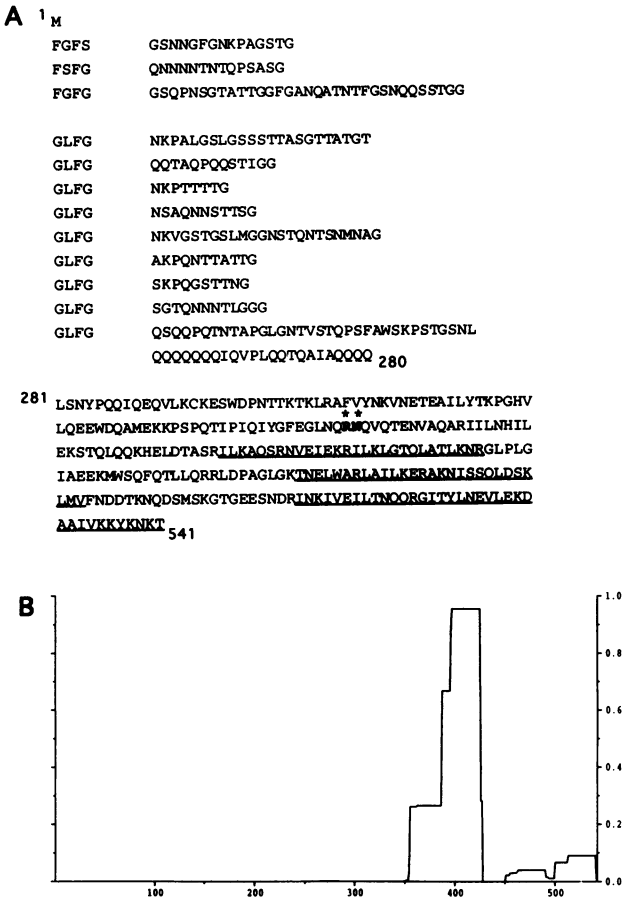

Fig. 1. Cloning and sequence analysis of *NUP57*. (**A**) Predicted amino acid sequence of the Nup57 protein and alignment of the three FXFG and nine GLFG repeat sequences; underlined are three longer sequences within the C-terminal domain which have heptad repeats and could be involved in coiled-coil interactions. (**B**) Prediction of coiled-coil regions within Nup57p; the program PEPCOIL was used which identifies potential coiled-coil regions of protein sequences using the algorithm of Lupas *et al.* (1991). The two asterisks indicate the two amino acids mutated in the sl29 mutant.

methods) and gave a temperature-sensitive phenotype (data not shown). This viable mutant nup57Δ enabled us to analyse the expression of Nup57p by Western blotting using a specific antibody against a C-terminal Nup57p peptide. On Western blots of whole yeast cell extracts of a wild-type strain, this antibody recognized a single band of 54 kDa (Figure 2A). Conversely, a whole-cell extract derived from the nup57Δ strain probed on Western blot with the anti-Nup57p peptide antibodies lacked the 54 kDa band; instead, a weak 20 kDa band appeared which corresponded to a shortened C-terminal domain of the Nup57p (Figure 2A; see also Materials and methods). In parallel, a polyclonal immune serum was raised against GLFG repeat sequences which recognizes on immunoblots the GLFG nucleoporins Nup116p, Nup100p, Nup57p and, to a lesser extent, Nup49p and the N-terminally cleaved form of Nup145p, called Nup145p-N (Fabre *et al.*, 1994; Figure 2B). Similarly, a Western blot of a whole-cell extract from the nup57Δ strain decorated with the anti-GLFG immune serum lacked the Nup57p band (Figure 2B). To confirm that Nup57p is the p54 protein present in the purified Nsp1p complex (Grandi *et al.*, 1993), a

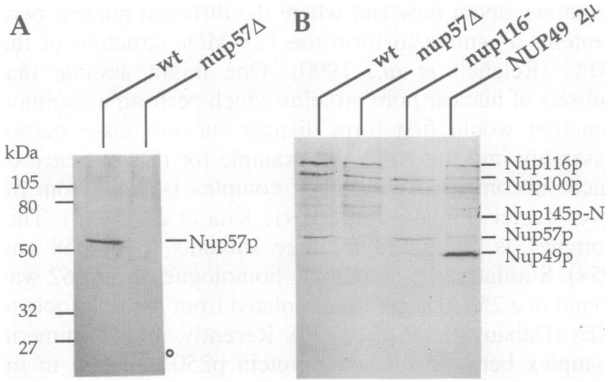

Fig. 2. Nup57p is the fifth cloned GLFG nucleoporin in yeast. (**A**) Immunoblot analysis of whole-cell extracts of wild-type *NUP57* (wt) and *HIS3::nup57* deletion/disruption strain (nup57Δ). The blot was probed with a polyclonal immune serum raised against a C-terminal peptide of Nup57p. The open circle (○) indicates a truncated C-terminal domain of Nup57p which is expressed in the nup57Δ strain. The molecular weight of a protein standard is given. (**B**) Immunoblot analysis of whole-cell extracts of a wild-type (wt), *HIS3::nup57* disrupted (nup57Δ), *nup116::URA3* disrupted (nup116$^-$) and Nup49p-overexpressing strain (NUP49 2μ, high-copy number plasmid). Equivalent amounts of extract were analysed by SDS–PAGE and immunoblotting. The GLFG nucleoporins were visualized using polyclonal antibodies raised against GLFG repeat sequences.

corresponding Western blot was probed with an anti-Nup57p peptide antibody. The band previously assigned to be the p54 component of the complex (Grandi *et al.*, 1993) was recognized by the anti-Nup57p antibody (data not shown). To demonstrate further that Nup57p is associated with the other members of the Nsp1p complex, we expressed the Nup57p C-terminal domain tagged with Protein A in yeast, and subsequently purified ProtA–Nup57p under non-denaturing conditions by IgG–Sepharose affinity chromatography. The silver-stained SDS–polyacrylamide gel showed that the purified fraction contains only a few bands, the most prominent one being the Nic96 protein. By Western blotting, Nsp1p (which is degraded during the purification procedure yielding several degradation products) also co-enriched during ProtA–Nup57p affinity purification (data not shown). Unfortunately, Nup49p cannot be distinguished clearly on this immunoblot because it migrates close to ProtA–Nup57p on SDS–polyacrylamide gels.

In summary, Nup57p is the previously described GLFG containing p54 component (Wente *et al.*, 1992), and is arranged together with Nsp1p, Nup49p and Nic96p in an NPC subcomplex (Grandi *et al.*, 1993). This complex, whose components are all essential for cell viability, is thus characterized both biochemically and genetically; strikingly, *in vitro* and *in vivo* data corroborate each other.

Mutations in the C-terminal domains of Nic96p and Nup57p cause synthetic lethality with ts Nsp1p

To gain an insight into the molecular mechanism by which synthetic lethality was generated, the sl alleles of *NIC96* and *NUP57* were recovered from the corresponding sl strains (sl57 and sl316 for *NIC96*; sl29 for *NUP57*). Strikingly, the two different *nic96* sl alleles carry a frame-shift mutation that generates proteins truncated in the C-

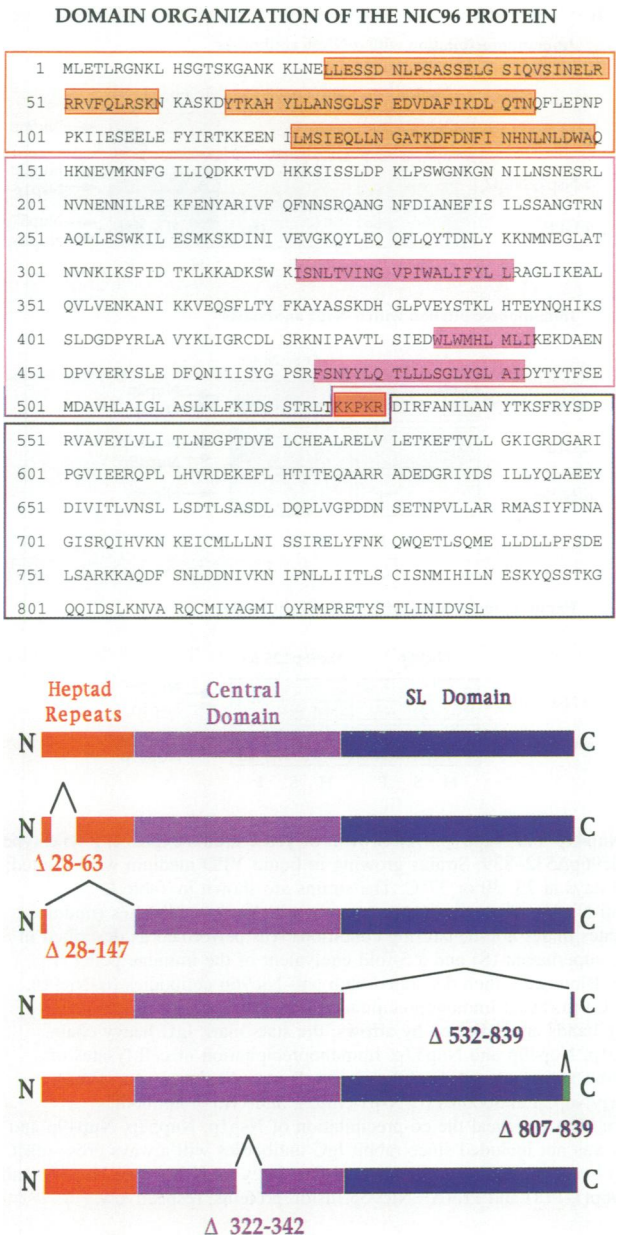

Fig. 3. Mutational analysis of the different Nic96p domains. Upper panel: amino acid sequence of the Nic96 protein. The N-terminal domain (surrounded in orange) exhibits three longer sequences with heptad repeat organization (i.e. disposition of hydrophobic residues at positions 1 and 4 of a seven residue-long repeat sequence; boxed in orange). The central domain (surrounded in violet) has three longer stretches of uncharged amino acids (boxed in violet) and a putative NLS (surrounded in red). The C-terminal domain (surrounded in blue) does not exhibit any particular feature. Lower panel: schematic representation of the Nic96p domain organization in heptad repeats (orange), central domain (violet) and the sl domain (blue), and mutants with the indicated deletions in the corresponding domains.

terminal domain (see Materials and methods). In the case of sl57, the last 30 amino acids were deleted, but an additional unrelated 20 amino acids were added due to a shift in another short open reading frame (ORF; Figure 3, Nic96pΔ807–839); in the case of sl316, the last 252 C-terminal amino acids were removed. When these mutant alleles, *nic96-57* and *nic96-316*, were inserted into a yeast single-copy number plasmid and transformed in the corresponding sl mutants, they could not rescue the sl phenotype although they were expressed in similar amounts as compared with intact Nic96p (data not shown). On the other hand, both sl alleles efficiently complemented the *nic96* null mutant in a background of wild-type *NSP1* at 23 and 30°C; at 37°C, the *nic96-316* allele was growing slightly slower compared with a wild-type *NIC96* (data not shown).

The recovered *nup57* sl allele from strain sl29 revealed the presence of two mutations (R361 → P and N362 → Y) which map within the essential C-terminal domain but outside the predicted coiled-coil region (Figure 1A). The *nup57-29* allele did not complement the sl29 mutant strain but was functional, since it complemented the nup57 disruption mutant (data not shown).

Nic96p has several distinct functional domains

The primary amino acid sequence of Nic96p can be roughly divided into three domains: (i) the N-terminal part which contains heptad repeats, as found in the C-terminal domains of Nsp1p, Nup49p and Nup57p; (ii) an adjacent central domain with several stretches of hydrophobic amino acids, and (iii) a 310 amino acid long C-terminal domain that does not reveal any particular sequence motif in its primary sequence (Figure 3).

In an attempt to assign specific functions to these various Nic96p domains we generated nested deletions. First, we analysed the role of the heptad repeats within the Nic96p N-terminal domain. Two constructs were generated, Nic96pΔ28–63 and Nic96pΔ28–147, in which respectively one third and the entire coiled-coil part was removed (Figure 3). The deletion mutant Nic96pΔ28–63, although viable at permissive temperatures, is impaired in cell growth and stops growing at 37°C (Figure 4A). This growth defect is enhanced further when the entire heptad repeat domain is deleted because cells grow very slowly even at permissive temperatures (Figure 4A). The heptad repeats in Nic96p thus perform a crucial function for yeast cell growth.

Since heptad repeats are present in all four members of the Nsp1 complex, it is likely that these parts are involved in protein–protein interaction, as shown for other heptad repeat-containing proteins such as nuclear lamins (McKeon *et al.*, 1986) and heterotrimeric G-proteins (Simonds *et al.*, 1993). To test whether the growth defect of Nic96pΔ28–63 cells parallels a defect in physical interaction between Nic96p and the other members of the complex, we performed immunoprecipitation under non-denaturing conditions using anti-Nic96p peptide antibodies. When a wild-type *NIC96* strain was used for immunoprecipitation, the immune pellet contained Nic96p, Nsp1p, Nup49p and Nup57p, but not Nup2p (Figure 4B, upper panel) or other nucleoporins (data not shown) which are absent from the Nsp1p-containing complex (Grandi *et al.*, 1993). The same result was obtained with the C-terminally truncated Nic96pΔ532–839 protein showing that this part is not required for physical interaction with the other nucleoporins (Figure 4B, upper panel). In contrast, no co-precipitation of Nsp1p, Nup49p or Nup57p was seen when Nic96pΔ28–63 was immunoprecipitated (Figure 4B, upper panel).

The lack of physical association of Nic96pΔ28–63 with the other members of the complex could mean that the whole complex has dissociated or Nic96pΔ28–63 is

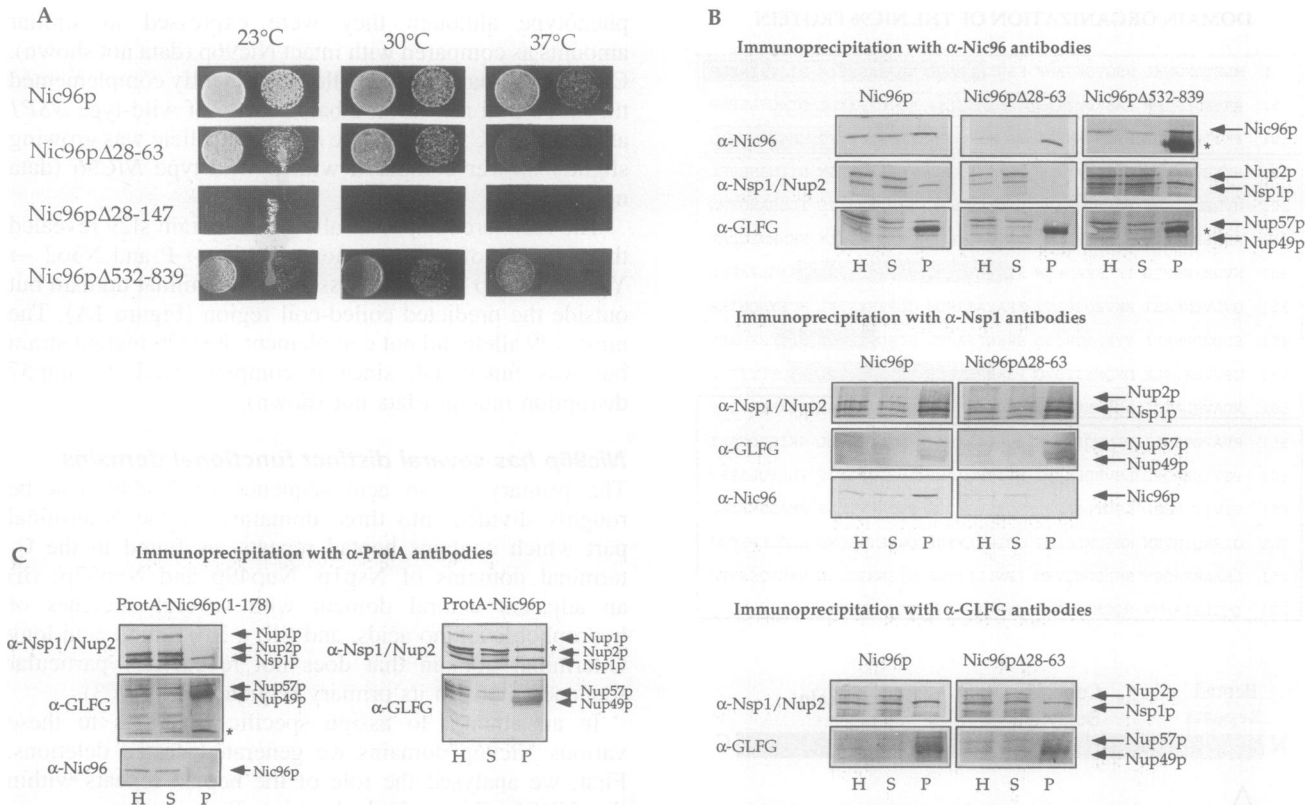

Fig. 4. The heptad repeats in Nic96p are required for association with Nsp1p, Nup49p and Nup57p. **(A)** Growth of yeast strains expressing wild-type Nic96p and various deletion constructs: Nic96pΔ28–63, Nic96pΔ28–147 and Nic96pΔ532–839. Strains growing in liquid YPD medium were diluted; 5 μl of the diluted suspensions were applied on YPD plates and incubated for 3 days at 23, 30 or 37°C. The strains are shown in Table I. **(B)** Immunoprecipitation from wild-type and Nic96 mutant cell lysates using anti-Nic96p antibodies (upper panel), anti-Nsp1p antibodies (middle panel) and anti-GLFG antibodies (lower panel). Immunoprecipitation of cell lysates under non-denaturing conditions was performed as described in Materials and methods. A 1-fold equivalent of the homogenate (H) and immune supernatant (S) and a 5-fold equivalent of the immune pellet (P) were separated on SDS–polyacrylamide gels before blotting onto nitrocellulose. Blots were then decorated with anti-Nic96p antibodies (α-Nic96), anti-Nsp1p/Nup2p antibodies (α-Nsp1/Nup2) and anti-GLFG antibodies (α-GLFG) to reveal immunoprecipitation of Nic96p and co-immunoprecipitation of Nsp1p, Nup2p, Nup57p and Nup49p. The corresponding bands are indicated by arrows; the stars mark IgG heavy chain. **(C)** The heptad repeats of Nic96p can bind to a core complex consisting of Nsp1p, Nup49p and Nup57p. Immunoprecipitation of cell lysates of NIC96 shuffle strain expressing ProtA–Nic96p(1–178) and ProtA–Nic96p. Rabbit anti-chicken IgGs followed by ProtA–Sepharose (α–ProtA antibodies) were used for immunoprecipitation of the fusion proteins. Anti-Nsp1p/Nup2p antibodies (α-Nsp1/Nup2), anti-GLFG antibodies (α-GLFG) and anti-Nic96p antibodies (α-Nic96) were used to probe the Western blots to reveal the co-precipitation of Nsp1p, Nup57p, Nup49p and Nic96p. In the case of ProtA–Nic96p, re-decoration with anti-Nic96 antibodies was not included since rabbit IgG antibodies will always cross-react with the ProtA moiety of the full-length Nic96p fusion protein. The nucleoporin bands are indicated by arrows. The fuzzy band between Nup57p and Nup49p is IgG heavy chain. The stars indicate the positions of the ProtA–Nic96p(1-178) and ProtA–Nic96p fusion proteins, respectively.

specifically detached from a Nsp1p–Nup49p–Nup57p core complex under immunoprecipitation conditions. To distinguish between these possibilities, we performed immunoprecipitation with anti-Nsp1p (Figure 4B, middle panel) and anti-GLFG antibodies (Figure 4B, lower panel) in a wild-type strain and in a strain expressing Nic96pΔ28–63. In both strains, Nsp1p, Nup49p and Nup57p always co-immunoprecipitated, whereas the mutant protein Nic96pΔ28–63 was absent under these conditions (Figure 4B, middle and lower panels). This shows that the partial deletion of the N-terminally located heptad repeats of Nic96p prevents the stable association with an Nsp1p–Nup49p–Nup57p core complex. Consistent with this observation is the fact that transcriptional repression of *NIC96* did not affect the expression and stability of the other nuclear pore proteins (e.g. Nsp1p and Nup49p) which were detected in normal amounts, although Nic96p was no longer synthesized (data not shown).

Similarly, mutations in the heptad repeats of a core member of the complex, e.g. mutation in the Nup49p C-terminal domain (Doye *et al.*, 1994), did not inhibit co-immunoprecipitation of Nsp1p and Nup57p, but Nic96p was again no longer associated with the core complex (Figure 5). A tagged version of the Nsp1p mutant Ala6-nsp1p, in which six charged amino acids within two heptad repeats were changed into alanines (Wimmer *et al.*, 1993), could also no longer interact with Nic96p (Grandi *et al.*, 1993).

The efficiency of immunoprecipitation of Nic96p or Nsp1p in these experiments varied to a certain extent, but was generally between 20 and 30%. However, if the immune supernatant was subjected to another round of immunoprecipitation, about the same amount of Nic96p and Nsp1p, respectively, and its co-precipitating proteins found previously in the first immune pellet, were recovered in the second immunoprecipitate (data not shown). This shows that the availability of antibodies is rate-limiting in immunoprecipitation rather than there being different populations of Nic96p- or Nsp1p-containing protein complexes.

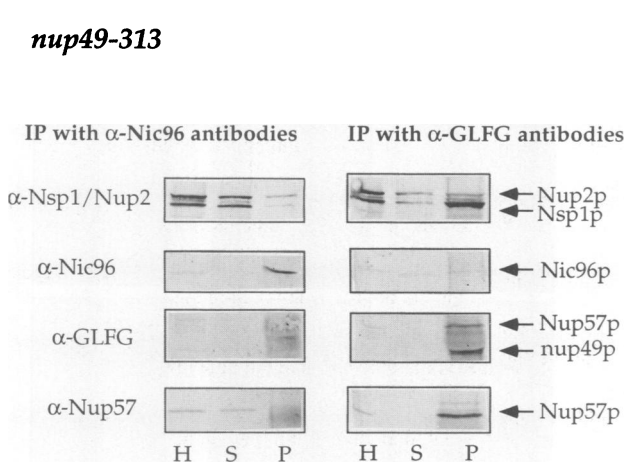

Fig. 5. Mutations in the essential C-terminal domain of Nup49p allow core complex formation but impair interaction with Nic96p. Immunoprecipitation from strain *nup49-313* that carries mutations in the essential C-terminal domain (Doye *et al.*, 1994), using anti-Nic96p antibodies (left panel) and anti-GLFG antibodies (right panel). Immunoprecipitation of cell lysates under non-denaturing conditions was performed as described in Materials and methods. Aliquots of the homogenate (H), immune supernatant (S) and immune pellet (P) were separated on SDS–polyacrylamide gels before blotting onto nitrocellulose. Blots were decorated with anti-Nsp1p/Nup2p antibodies (α-Nsp1/Nup2), anti-Nic96p antibodies (α-Nic96), anti-GLFG antibodies (α-GLFG) and anti-Nup57p antibodies (α-Nup57) to reveal immunoprecipitation and co-immunoprecipitation. Nucleoporin bands are indicated by arrows.

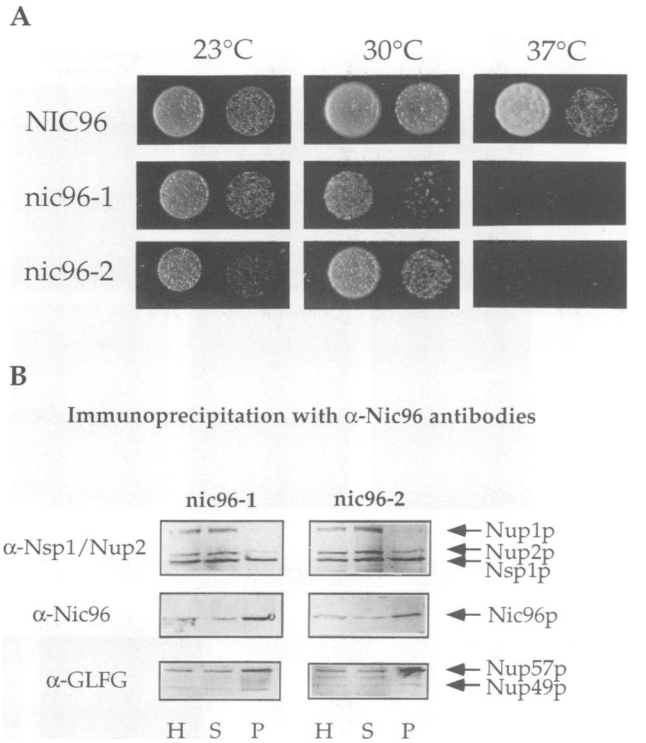

Fig. 6. Temperature-sensitive mutants of Nic96p which map in the central domain. (**A**) Growth phenotype of the ts mutants which map in the central domain of Nic96p. Dilutions of wild-type and nic96-1/nic96-2 mutant strains were performed as described in the legend to Figure 4A and incubated for 3 days at 23, 30 and 37°C. The strains were named as shown in Table I. (**B**) Immunoprecipitation from nic96-1 and nic96-2 cell lysates using anti-Nic96p antibodies under non-denaturing conditions as described in Materials and methods. Aliquots of the homogenate (H), immune supernatant (S) and immune pellet (P) were separated on SDS–polyacrylamide gels before blotting onto nitrocellulose. Blots were decorated with anti-Nsp1p/Nup2p antibodies (α-Nsp1/Nup2), anti-Nic96p antibodies (α-Nic96) and anti-GLFG antibodies (α-GLFG) to reveal immunoprecipitation and co-immunoprecipitation. Nucleoporin bands are indicated by arrows.

To obtain positive evidence that the coiled-coil part of Nic96p can bind directly to the heterotrimeric nucleoporin complex, only the heptad repeat domain of Nic96p (residues 1–178; see also Figure 3) tagged with Protein A was expressed in yeast. Since ProtA–Nic96p(1–178) did not complement the nic96 null mutant (data not shown), the construct was expressed in a wild-type *NIC96* background. Following immunoprecipitation under non-denaturing conditions, Nsp1p, Nup49p and Nup57p, but not full-length Nic96p, were found in the immune pellet together with ProtA–Nic96p(1–178) (Figure 4C). In a control experiment, immunoprecipitation of ProtA–DHFR did not co-precipitate these nucleoporins (data not shown). We therefore conclude that the heptad repeat domain of Nic96p alone can bind to the heterotrimeric nucleoporin complex.

The primary sequence of the central part of Nic96p is characterized by several longer stretches of uncharged amino acids, the most conspicuous one between residues 322 and 342 (Figure 3). To analyse the *in vivo* role of this hydrophobic sequence, the DNA encoding these 20 amino acids was removed from the *NIC96* gene. The resulting mutant protein, nic96pΔ322–342 (Figure 3) is not functional and cannot complement a *nic96* null mutant (data not shown). To gain further insight into the role of the central domain of Nic96p, mutations were generated in this part which resulted in ts *nic96* variants. We chose a PCR approach (Morrison and Desrosiers, 1993) that would introduce planned mutations between residues 322 and 342, as well as random mutations due to the PCR amplification within a longer fragment of the central domain of Nic96p (see also Materials and methods). Two ts *nic96* alleles were isolated (termed *nic96-1* and *nic96-2*) which could grow at 23 and 30°C, but not at 37°C (Figure 6A). The nic96-1 mutant stops cell growth by 6 h after the shift to 37°C, whereas it takes ~12 h for nic96-2. Sequencing of the ts alleles revealed that in *nic96-1*, proline 332 was changed to leucine, and leucine 260 to proline; in *nic96-2*, tryptophan 334 was changed to arginine.

To characterize the biochemical properties of these two ts Nic96 proteins, we performed immunoprecipitations identical to those carried out for the deletion mutant lacking part of the heptad repeats (also a ts mutant; see also Figure 4A). In contrast to Nic96pΔ28–63, both Nic96p(P332 → L, L260 → P) and Nic96p(W334 → R) could still interact with the other components of the complex, even if cells were incubated for 7 h at 37°C prior to immunoprecipitation (Figure 6B). These data show that the ts phenotype of the *nic96-1* and *nic96-2* alleles is not due to a dissociation of mutant Nic96p from the core complex.

The C-terminal domain of Nic96p (~300 amino acids in length) is not essential for cell viability, and its complete removal causes only a slight decrease in cell viability at 37°C (Figure 4A). As shown by immunoprecipitation of the Nic96pΔ532–839, removal of the C-terminal domain of Nic96p still allows complex formation with Nsp1p,

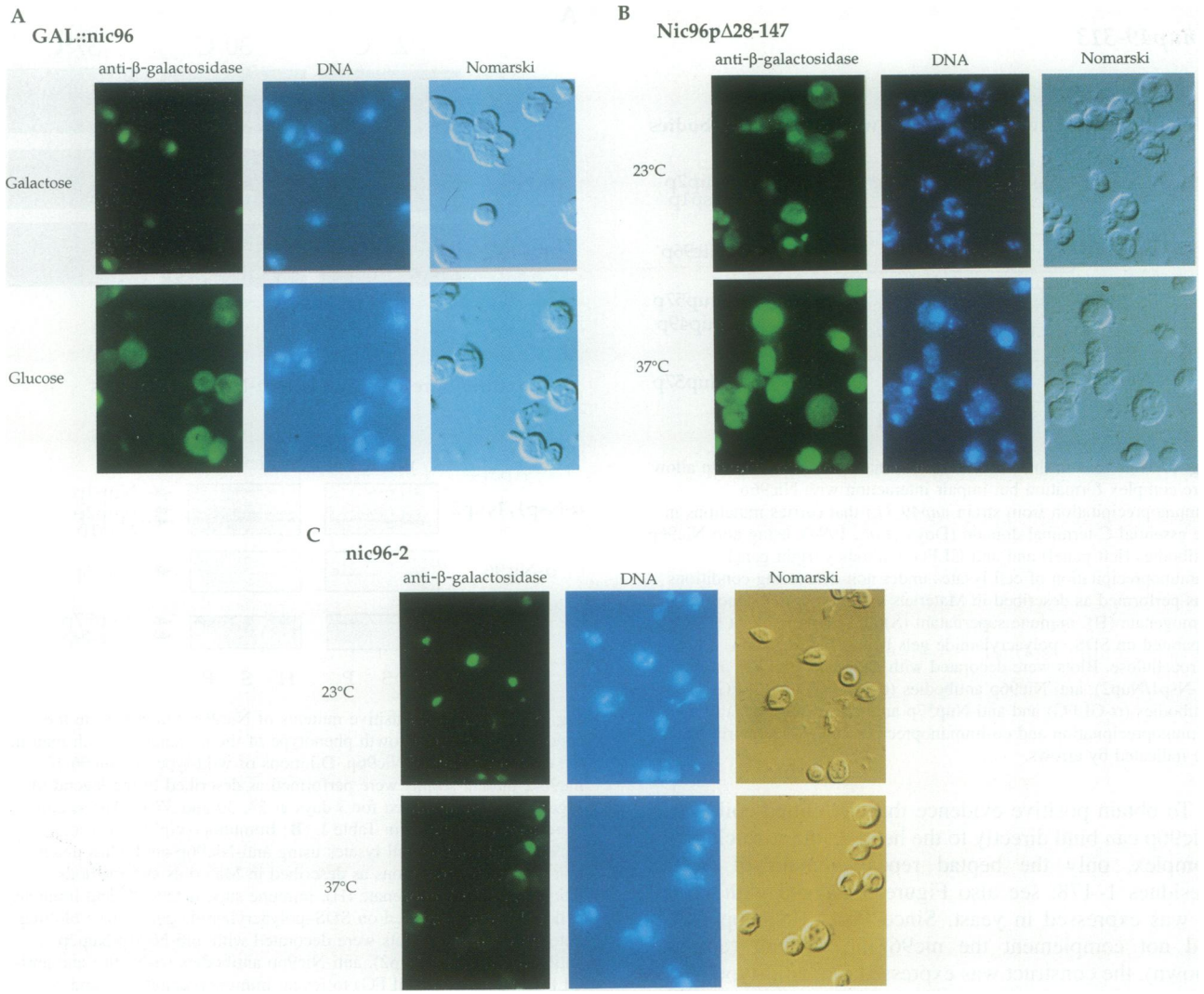

Fig. 7. Nucleocytoplasmic transport in Nic96p mutants. The *GAL::nic96* strain, NIC96 shuffle strain expressing Nic96Δ28–147p and nic96-2 strain were transformed with the plasmid YEp13::Matα2Δ(2–135)−lacZ which encodes a fusion protein between the yeast transcriptional repressor Matα2 and *Escherichia coli* β-galactosidase. (**A**) *GAL::nic96* cells were grown first in selective galactose medium and then transferred to selective glucose medium. After 8 h in glucose, cells were fixed in 3% formaldehyde and processed for indirect immunofluorescence using a mouse monoclonal antibody against lacZ, as described in Materials and methods. NIC96 shuffle strain expressing Nic96pΔ28–147 (**B**) and nic96-2 strain (**C**) were grown first in selective glucose medium at 23°C before transfer to 37°C for 6 (**B**) and 11 h (**C**). Representative photographs which show the location of the nuclear reporter protein (Matα2−lacZ) were put together. Also nuclear DNA staining and Nomarski optics are shown.

Nup49p and Nup57p (Figure 4B). Similarly, when the Nic96pΔ807–839 and Nic96pΔ587–839 proteins derived from the sl57 and sl316 mutants were expressed in a ProtA−Nsp1p-expressing strain followed by affinity purification of ProtA−Nsp1p, both shortened forms of Nic96p could be recovered efficiently in the purified Nsp1p complex (data not shown).

To test whether truncations in the C-terminal domain of Nic96p give rise to synthetic lethality when combined with mutants of other members of the complex, we combined the *nic96-316* sl allele with the *nup57Δ* allele. Haploid cells carrying both mutations are not viable, i.e. they are sl (data not shown). We conclude that the C-terminal domain of Nic96p, although not involved directly in the association with the nucleoporin complex, becomes essential when individual members are mutated (see also Discussion).

Nucleocytoplasmic transport in NIC96 mutants

To analyse whether Nic96p is involved in nucleocytoplasmic transport, we tested both import of a nuclear reporter protein, Matα2−lacZ, into the nucleus and distribution of poly(A)$^+$ RNA in nic96 mutant strains. We used a *GAL::nic96* strain in which the expression of the *NIC96* gene is repressed in glucose-containing medium and accordingly cells stopped growing after 10 h (data not shown). When *GAL::nic96* cells expressing the fusion protein Matα2−lacZ were grown for 8 h in glucose, cytoplasmic mislocalization of the nuclear reporter protein was seen (Figure 7A). A similar defect in nuclear uptake of Matα2−lacZ was also observed for the nic96 mutant lacking one third (Nic96pΔ28–63; data not shown) or all of the heptad repeats (Nic96pΔ28–147; Figure 7B) when shifted to the non-permissive temperature. Interestingly, in the Nic96pΔ28–147 mutant the beginning of cytoplasmic

mislocalization of Matα2−lacZ was already observed at the permissive temperature (Figure 7B), consistent with the very slow growth of this mutant strain at 23°C (see also Figure 4A).

Import of Matα2−lacZ was analysed further in nic96 mutant strains carrying point mutations in the central domain (see also Figures 3 and 6B). In contrast to *GAL::nic96* and the strain carrying a deletion in the heptad repeats of Nic96p, ts nic96-1 cells shifted for 6 h to 37°C (data not shown), and nic96-2 cells shifted for 11 h to 37°C (Figure 7C), were not impaired in the nuclear uptake of Matα2−lacZ (see also Discussion).

When distribution of poly(A)$^+$ RNA was tested in *GAL::nic96* cells depleted of Nic96p for 8 h in glucose medium, poly(A)$^+$ RNA did not accumulate inside the nucleus and was normally distributed in the cytoplasm (data not shown). Another nucleoporin mutant *GAL::nup145* shows under the same conditions significant poly(A)$^+$ RNA accumulation inside the nucleus (Fabre *et al.*, 1994). Since mutations in other core members of the Nsp1 complex cause accumulation of nuclear reporter proteins in the cytoplasm (see also Discussion), it seems that this NPC subcomplex is required for the import of the karyophilic reporter protein into the nucleus.

Discussion

In this study we provided evidence that the four nucleoporins Nsp1p, Nup49p, Nup57p and Nic96p are both genetically and biochemically linked to each other. To unravel the molecular mechanism which drives the formation of this essential NPC subcomplex *in vivo*, we started to analyse by immunoprecipitation how Nic96p, an abundant nuclear pore complex protein in yeast, participates in the interaction with its partner proteins. However, it should be kept in mind that this biochemical approach only allows us to conclude whether protein−protein interactions are stable in the test tube after cell breakage, and does not reflect the stage of interaction within the living cell. We have not been able to compare these biochemical data with *in vivo* location studies because the anti-Nic96 peptide antibodies used in this study are not reactive in indirect immunofluorescence.

A structural motif common to all four members of the complex is the occurrence of heptad repeats. Interestingly, we found that although deletions in the heptad repeat domain of Nic96p impair interaction with the other nucleoporins, a core complex consisting of Nsp1p, Nup49p and Nup57p could still be isolated biochemically. However, the heptad repeats within Nic96p are not absolutely required for the essential function because Nic96pΔ28–147 can support growth at lower temperatures, albeit very slowly. Thus, Nic96p lacking its heptad repeats may still interact *in vivo* to a certain extent with the Nsp1p−Nup57p−Nup49p core complex or, alternatively, the core complex could be weakly bound to NPC components other than Nic96p.

Mutation in the coiled-coil domain of a core complex member (e.g. Nup49p or Nsp1p), which impairs the *in vivo* function but still allow core complex formation, also disturbs the biochemical interaction with Nic96p. Thus, Nic96p easily dissociates from a biochemically stable Nsp1p−Nup49p−Nup57p core complex whose assembly is less sensitive to mutational perturbation. This may be because of the different structural organization of Nic96p as compared with Nsp1p, Nup49p and Nup57p. Moreover, while for Nsp1p, Nup49p and Nup57p the heptad repeat-containing C-terminal domains contain all the essential features for NPC targeting and association (Hurt, 1990; Nehrbass *et al.*, 1990; Wimmer *et al.*, 1992; Grandi *et al.*, 1993; this work), these functions cannot be restricted to the heptad repeats in Nic96p. For a functional Nic96p, both the N-terminal heptad repeat domain and the adjacent central domain are required in concert.

Since it has been shown that higher eukaryotic p62 is homologous to Nsp1p (Carmo-Fonseca *et al.*, 1991), it might be that p58 and p54, which seem to be FXFG/GLFG-containing components of the p62 complex (Rout and Wente, 1994), correspond to yeast Nup57p and Nup49p. If the yeast Nsp1p and higher eukaryotic nucleoporin p62 perform a similar evolutionarily conserved function, one wonders why the mammalian complex apparently lacks a corresponding Nic96p homologue. It may be that a homologous Nic96p is less tightly bound to the mammalian p62−p58−p54 complex and, therefore, might easily dissociate during purification.

What could be the function of the central domain of Nic96p? Although hydropathy plot analysis reveals that the 20 amino acid-long uncharged sequence resembles membrane-spanning sequences, biochemical evidence suggests that Nic96p is not an integral membrane protein (P.Grandi, unpublished results). The mutant alleles in the central domain of Nic96p which confer a ts phenotype are worth mentioning in this context. In one case, proline mutations may have altered the secondary structure of this part of Nic96p; in the other case, a tryptophan residue (335) was converted into a positively charged arginine which disrupts the continuity of the essential hydrophobic stretch. It is therefore possible that these mutations affect the overall folding of the central domain which may be the part in Nic96p that mediates binding to the NPC. However, further experimental work is required to show that the central domain of Nic96p is involved in docking to the NPC, thereby exposing the adjacent heptad repeats which themselves can bind to the nucleoporin core complex. Since Nic96p is an abundant component of the NPC, it might not only interact with the Nsp1p−Nup49p−Nup57p complex, but could also be a docking site for other NPC components. Recently, a biochemical method was described which allowed the isolation of highly purified yeast NPCs (Rout and Blobel, 1993). Nic96p co-purifies with these NPCs during the enrichment procedure (M.Rout and G.Blobel, personal communication) and represents a prominent nuclear pore component accounting for some 8 MDa, which is up to 10 copies of Nic96p per spoke (Rout and Wente, 1994).

It is striking that a 30 amino acid deletion from the Nic96p C-terminal domain is fully functional in an *NSP1*$^+$ genetic background but causes such a drastic defect (i.e. sl) with a ts allele of *nsp1* which has a single L → S substitution within the C-terminal domain. Since the nup57Δ mutant exhibits a similar sl phenotype with C-terminal truncations of Nic96p, no allele specificity exists; accordingly, the interaction/assembly of Nic96pΔ807–839 with a mutated but not intact Nsp1p−Nup49p−Nup57p core complex as a whole may be impaired. We therefore

speculate that the Nic96p C-terminal domain facilitates in a chaperonine-like fashion the association of the essential Nic96p N-terminal domain with the core nucleoporin complex. Alternatively, the Nic96p C-terminal and the Nsp1/Nup57p C-terminal domain(s) fulfil a redundant, overlapping function.

What could be the overall function of the nucleoporin complex studied in this work? Mutations in components of the core complex (e.g. Nsp1p and Nup49p), as well as (partial) deletion of the heptad repeats from Nic96p which mediate interaction with the core complex, can cause cytoplasmic accumulation of nuclear localization sequence (NLS)-containing reporter proteins (Nehrbass *et al.*, 1993; Schlenstedt *et al.*, 1993; Doye *et al.*, 1994; this work). It is still not clear whether these NPC components are involved directly in nuclear protein import. Should they, however, play a direct role, it is tempting to speculate that the core complex is located at the cytoplasmic side of the NPC, where it could possibly interact with (cytoplasmic) factors involved in protein import into the nucleus. Indeed, Nsp1p seems to be available for the binding of specific antibodies on the cytoplasmic side of the NPC (Schlenstedt *et al.*, 1993). It is also worth mentioning that mammalian p62 can bind to a soluble factor required for nuclear protein import (L.Gerace, personal communication). On the other hand, Nic96p may perform additional roles at the NPC, e.g. being a crucial structural component of the NPC or a substructure of the NPC (see also above). Since ts Nic96p mutants which map in the central domain apparently do not accumulate the nuclear reporter protein in the cytoplasm at the non-permissive temperature, this part of Nic96p could perform (an) additional function(s) not related to nuclear protein uptake. Therefore it will be interesting to determine which other components of the NPC functionally interact with the central domain of Nic96p; genetic screens are under way to study this question.

Between the central and the C-terminal domains of Nic96p is a short, positively charged amino acid sequence (KKPKR; see also Figure 3) which is reminiscent of a NLS. When this sequence was fused to *Escherichia coli* β-galactosidase and the corresponding fusion protein expressed in yeast, it was targeted into the nucleus (P.Grandi, unpublished results). Interestingly, none of the other components of the Nsp1 complex contain canonical NLSs in their primary amino acid sequences. Experiments are under way to find out whether this Nic96p NLS could contribute to the nuclear targeting of the whole nucleoporin complex before assembly into the NPC.

Combining our genetic and biochemical data, we think that the NPC is built up of functionally distinct subcomplexes. Since there are a large number of different functions to be fulfilled by the nuclear pore complex, we believe that other subcomplexes remain to be identified and characterized. Synthetic lethal screens combined with biochemical approaches represent a powerful way of cloning new nuclear pore components and studying the structural relationships and functional interactions between them.

Materials and methods

Yeast strains, media and microbiological techniques

The strains used in this study are listed in Table I. Microbiological techniques, including yeast growth on minimal and rich YPD medium, plasmid transformation, gene disruption, sporulation of diploid cells and tetrad analysis, were performed essentially as described in Wimmer *et al.* (1992), with the exception that in most cases the minimal SD medium was supplemented by all amino acids and nutrients except those used for selection (CSM medium, BIO101, La Jolla, CA); where appropriate, 5-FOA (Jersey Laboratory Supplies) was added.

Plasmids

The following yeast plasmids were used in this study: pUN100, *ARS/CEN* plasmid with the *LEU2* marker (Elledge and Davis, 1988); pRS414, *ARS/CEN* plasmid with the *TRP1* marker (Sikorski and Hieter, 1989); pRS315, *ARS/CEN* plasmid with the *LEU2* marker (Sikorski and Hieter, 1989); pRS316, *ARS/CEN* plasmid with the *LEU2* marker (Sikorski and Hieter, 1989); pCH1122, YCp50 derivative (*ARS/CEN* 4) with the *URA3* and *ADE3* markers (Kranz and Holm, 1990); YEp13, 2μ plasmid with the *LEU2* marker; pRS414-ts nsp1L → S (Wimmer *et al.*, 1992); pUN100-NIC96 (Grandi *et al.*, 1993); YEp13-ProtA−DHFR (Grandi *et al.*, 1993); YEp13-Matα2−lacZ (Nehrbass *et al.*, 1993).

Isolation of synthetic lethal mutants of ts nsp1

Synthetic lethal mutants of a ts nsp1 allele were isolated essentially as described earlier (Wimmer *et al.*, 1992), with the exception that strain RW24-1 was used which contains both the genomic plus an extra ARS/CEN plasmid-linked copy of the *NUP116* and *NUP49* genes. 110 000 colonies which survived the UV mutagenesis were screened for a red, non-sectoring phenotype. A total of 14 new sl mutants was isolated from this extended screen and characterized according to Wimmer *et al.* (1992). These 14 non-sectoring sl mutants were finally transformed with pUN100-NIC96; two synthetic lethal strains, sl57 and sl316, were complemented by the *NIC96* gene, i.e. they displayed a red/white sectoring phenotype and could grow on 5-FOA-containing plates.

Cloning, sequencing and disruption of the NUP57 gene

A yeast genomic library inserted into pUN100 was transformed into one of the new sl mutants, sl29, as described earlier (Wimmer *et al.*, 1992). Transformants which showed red/white sectoring and growth on 5-FOA were obtained and the complementing plasmid was recovered by isolation of total yeast DNA and transformation of *E.coli*-competent MC1061 cells. A pUN100 plasmid containing a 10 kb insert was recovered which, if re-transformed in sl29, conferred complementation. Subcloning of restriction fragments showed that the complementing activity was restricted to a 4.5 kb *Hin*dIII−*Eco*RI fragment; furthermore, deletion of an internal 0.45 kb *Bam*HI−*Bam*HI fragment within the 4.5 kb *Hin*dIII−*Eco*RI fragment abolished complementation. The 4.5 kb *Hin*dIII−*Eco*RI fragment was subcloned into pBluescript KS; 2.5 kb of it, including the entire *NUP57* gene, were sequenced on both strands according to Sanger *et al.* (1977) using M13 universal and reverse, as well as internal, primers. DNA and deduced amino acid sequences were analysed by the GCG programs and the molecular weight by the PEPTIDESORT program. 3′ to the *NUP57* gene is the gene encoding the S28 ribosomal subunit (GenBank accession number M96570).

To disrupt the complete *NUP57* gene, two DNA fragments were first PCR-amplified corresponding largely to the 5′ non-coding region of *NUP57* (from position −375 to +57 relative to the ATG start codon, with a new *Eco*RI site generated at −375 and a *Bam*HI site at +57) and 3′ non-coding region of *NUP57* (from position +1537 to +1944 relative to the ATG start codon, with a new *Bam*HI site generated at +1537 and a *Sph*I site at +1944; the stop codon is at position +1625). The two PCR fragments were joined at their *Bam*HI sites (connecting nucleotide +57 with nucleotide +1537) and the derived *Eco*RI−*Sph*I fragment was inserted into pUC19. This construct was then cut open at the internal *Bam*HI site (at the +57/+1537 junction); the *HIS3* gene isolated as a 1.15 kb *Bam*HI fragment from plasmid YDpH was ligated into this site. The *nup57::HIS3* DNA was finally excised as an *Eco*RI−*Sph*I fragment, used to transform the diploid strain RS453 and HIS$^+$ transformants selected. Correct integration of this *nup57::HIS3* null allele at the *NUP57* gene locus was verified by Southern analysis. Strain NS1 heterozygous for *NUP57* was sporulated and tetrad analysis was performed using the MSM Singer tetrad dissection microscope.

Another *NUP57* gene disruption which gave expression of a truncated Nup57p C-terminal domain and caused a temperature-sensitive phenotype was performed as follows. The *HIS3* gene isolated as a 1.15 kb blunt-ended *Bam*HI fragment from plasmid YDpH was used to replace the 0.45 kb internal *Bam*HI−*Bam*HI fragment within the coding sequence of the *NUP57* gene (between Val153 and Asn302; see also Figure 1A). This linearized *nup57::HIS3* DNA was used to transform the diploid strain RS453, and HIS$^+$ transformants were selected. Correct integration

Table I. Yeast strains

Strain	Genotype
RS453	**a**/α, *ade2/ade2, trp1/trp1, leu2/leu2, ura3/ura3, his3/his3*
wt	α, *ade2, his3, leu2, trp1, ura3* (haploid derivative from RS453)
RW24-1	α, *ade2, ade3, leu2, trp1, ura3, nsp1::HIS3* [pCH1122-ADE3-URA3-NSP1, pRS414-TRP1-nsp1^{ts}(L640S)], pUN100-LEU2-NUP116-NUP49
PG1	**a**/α, *ade2/ade2, trp1/trp1, leu2/leu2, ura3/ura3, his3/HIS3::nic96* (Grandi *et al.*, 1993)
NIC96 shuffle	**a**, a*de2, trp1, leu2, ura3, HIS3::nic96* (pCH1122URA3-ADE3-NIC96); haploid progeny derived from PG1
GAL::nic96	**a**, *ade2, trp1, leu2, his3, URA3::GAL10::ProtA-NIC96*
nic96-1	**a**, *ade2, trp1, leu2, ura3, HIS3::nic96* [pUN100-LEU2-nic96^{ts}(P332L; L260P)]
nic96-2	**a**, *ade2, trp1, leu2, ura3, HIS3::nic96* [pUN100-LEU2-nic96^{ts}(W334R)]
sl57	α, *ade2, ade3, leu2, trp1, ura3, nsp1::HIS3, nic96-57* [pCH1122-ADE3-URA3-NSP1, pRS414-TRP1-nsp1^{ts}(L640S)]
sl316	α, *ade2, ade3, leu2, trp1, ura3, nsp1::HIS3, nic96-316* [pCH1122-ADE3-URA3-NSP1, pRS414-TRP1-nsp1^{ts}(L640S)]
sl29	α, *ade2, ade3, leu2, trp1, ura3, nsp1::HIS3, nup57-29* [pCH1122-ADE3-URA3-NSP1, pRS414-TRP1-nsp1^{ts}(L640S)]
NS1	**a**/α, *ade2/ade2, trp1/trp1, leu2/leu2, ura3/ura3, his3/HIS3::nup57* null
NS2	**a**/α, *ade2/ade2, trp1/trp1, leu2/leu2, ura3/ura3, his3/HIS3::nup57* deletion/disruption
nup57Δ	α, *ade2, trp1, leu2, ura3, HIS3::nup57* deletion/disruption
nup49-313	α, *ade2, ade3, his3, leu2, lys2, ura3, nup49::TRP1* (pUN90-nup49-313) (Doye *et al.*, 1994)

of this *nup57::HIS3* deletion/disruption allele at the *NUP57* gene locus was verified by Southern analysis and Western blotting. Strain NS2 heterozygous for *NUP57* was sporulated and tetrad analysis was performed. The reason for this partial gene disruption which gives expression of a truncated Nup57p is not known. We suspect that a promoter activity within the *HIS3* gene, which was inserted between amino acids Val153 and Asn302 of Nup57p, drives the expression of a Nup57p C-terminal domain starting at a new ATG codon (e.g. methionine 339; see also Figure 1A).

Construction of ProtA–Nup57p

The DNA encoding the C-terminal domain of Nup57p (starting from residue Asn238) was amplified by PCR using two primers which created a new *Eco*RI site at the 5′ end and a *Xba*I site at the 3′ end of the *NUP57* gene. In a triple ligation, the resulting 1 kb *Eco*RI–*Xba*I fragment was joined with a *Hin*dIII–*Eco*RI fragment corresponding to a *NOP1* promoter–ProtA construct (Bergès *et al.*, 1994) in the vector pRS316, opened at its *Hin*dIII–*Xba*I sites. At the *Eco*RI site the ProtA was fused in-frame to the C-terminal domain of Nup57p. The resulting plasmid pRS316–ProtA–NUP57 was transformed into the nup57Δ strain. Whole-cell extracts from HIS$^+$/LEU$^+$ transformants were analysed by Western blotting for the expression of a 49 kDa fusion protein, and the ProtA–Nup57p was purified by IgG–Sepharose affinity chromatography as described in Grandi *et al.* (1993).

Generation of α-GLFG, α-Nup57 and α-Nic96 antibodies

Rabbit polyclonal anti-GLFG antibodies were generated using a bacterially expressed $(HIS)_6$–$(GLFG)_{22}$ fusion protein for the immunization. For this purpose, the DNA encoding most of the GLFG repeat domain of Nup116p was amplified from the *NUP116* gene by PCR using two internal primers [nucleotides 1090–2020 (see Wimmer *et al.*, 1992) and cloning of this DNA fragment into the pET-HIS6 vector (Studier *et al.*, 1990)]. The pET vector containing the fusion gene was transformed into *E.coli* BL21 cells and, after induction, the $(HIS)_6$–$(GLFG)_{22}$ fusion protein was extracted from the cell lysate and purified on a nickel column (Qiagen, Hilden, Germany).

To generate anti-Nic96 antibodies, the peptide Cys-Glu-Thr-Leu-Arg-Gly-Asn-Lys-Leu-His-Ser-Gly-Thr-Ser-Lys-Gly-Ala-Asn-Lys-Lys, corresponding to the first 20 N-terminal amino acids of Nic96p except the start methionine which was replaced by Cys, was used. For rabbit immunization, the peptide was coupled to keyhole limpet hemocyanin (KHL) via the N-terminal cysteine using the cleavable cross-linker SPDP (Pierce, Oud Beijerland, The Netherlands), as described in Carmo-Fonseca *et al.* (1991). The immune serum was finally affinity-purified against the Nic96 peptide coupled to a CNBr-activated Sepharose column. The same procedure was followed to obtain anti-Nup57p rabbit antibodies. In this case, a peptide derived from the extreme C-terminal end of the Nup57p, Cys-Glu-Val-Leu-Glu-Lys-Asp-Ala-Ala-Iso-Val-Lys-Lys-Tyr-Lys-Asn-Lys-Thr, was used.

Recovery of sl alleles

The mutated *nic96* genes which give raise to synthetic lethality in strains sl57 and sl316 (called *nic96-57* and *nic96-316*) were recovered by PCR. Total yeast genomic DNA prepared from these sl strains was used, and the amplification of the genes was performed by stepwise yielding of three PCR fragments covering the complete ORF of the *NIC96* gene. Each fragment was then subcloned into pBluescript for DNA sequencing (Sanger *et al.*, 1977). Since for both sl alleles mutations were only found in one of the three PCR fragments (corresponding to the Nic96p C-terminal domain), this DNA was replaced in the corresponding wild-type *NIC96* gene. In *nic96-57*, an extra nucleotide was inserted at position 2954 which shifted the ORF into another 25 bp-long ORF before running into a stop codon. The corresponding protein is called Nic96pΔ807–839. In *nic96-316*, a C → T nucleotide transition occurred at position 2296 which changed Leu587 to Phe; moreover, an adjacent extra nucleotide was inserted which shifted the *NIC96* ORF so that two further amino acid residues were generated before a stop codon terminated this truncated Nic96p (Nic96pΔ587–839). pUN100–nic96-57 and pUN100–nic96-316 were constructed by inserting the engineered *nic96-57* and *nic96-316* alleles (see above) into plasmid pUN100. These plasmids were re-transformed in strains sl57 and sl316, respectively, to confirm the plasmid-linked sl phenotype. The C-terminal part of the genomic *nup57* sl allele (called *nup57-29*) was recovered by PCR from strain sl29. This PCR fragment was fused in-frame to two IgG binding sequences of ProtA (see also above) and inserted into pRS314 to yield pRS314–ProtA–nup57-29. Sequencing of the *nup57* fragment of the fusion gene revealed two mutations: R361 → P and N362 → Y. pRS314–ProtA–nup57-29 was transformed into strains sl29 and nup57Δ to check for complementation.

Construction of nic96 mutant alleles

All PCR-derived constructs used in this study were routinely checked by DNA sequencing. To construct the pUN100–nic96Δ28–63 plasmid, an *Nhe*I restriction site was introduced by PCR in pUN100–NIC96 at nucleotide position 610 of the *NIC96* ORF, and the DNA fragment between this new *Nhe*I site and the existing *Nhe*I site at position 715 was removed (from Leu28 to Lys63). To construct pUN100–nic96Δ28–147, the pUN100–nic96Δ28–63 was used as template to introduce by PCR an additional *Nhe*I site at nucleotide position 970; the DNA sequence between nucleotide positions 610 and 970 was deleted (from Leu28 to Asp147).

The pUN100–nic96Δ532–839 was constructed by introducing the *Xba*I linker CTCTAGAG (New England Biolabs, Schwalbach/Taunus, Germany) at the *Eco*RV site within pUN100–NIC96 (Ile532), thereby creating a premature stop codon. To construct YEp13–ProtA–Nic96(1–178), a *Bam*HI–*Xba*I DNA fragment derived from pBluescript–ProtA–NIC96 (Grandi *et al.*, 1993), containing two IgG binding sequences of ProtA and the first 178 amino acids of Nic96p under the control of the *NOP1* promoter, was inserted into the *Bam*HI–*Xba*I-cut YEp13 vector. The resulting fusion protein carried nine additional amino acids at its C-terminal end which were derived from vector DNA sequences. Deletion of the hydrophobic sequence between residues 322 and 342 of Nic96p was carried out by introducing two new *Bam*HI restriction sites, corresponding to Ile322 and Leu341, and deleting the small internal *Bam*HI fragment between these residues. The resulting pUN100–nic96Δ322–342 exhibits the sequence Lys321-Gly-Ser-Arg343 in the corresponding region.

The ts *nic96-1* and *nic96-2* alleles were obtained by applying a

recently described PCR-mediated mutagenesis protocol (Morrison and Desrosiers, 1993) using two degenerated complementary oligonucleotides corresponding to the Nic96p protein sequence between residues Pro332 and Ala344: AAXGGGCCTTAAXATXTXATCXTTTAAGAGC and TCTTAAAAGAXAAAATAXAATGGCCCATATTGG (X = any nucleotide from a mixture T:C:G:A = 79:7:7:7). Two further internal non-mutagenic oligonucleotides, priming at positions 820 and 1850 respectively of the NIC96 gene sequence, were used in combination with the degenerated oligonucleotides. After PCR mutagenesis, the *NIC96* gene was cloned as a *XbaI−NdeI* restriction fragment in pUN100−NIC96, previously cut open at the matching *XbaI−NdeI* restriction sites. Thus, a plasmid library of mutants was generated which was transformed into the NIC96 shuffle strain. A total of 128 LEU^+ transformants were plated on 5-FOA at 23°C; 112 colonies which grew normally were checked for a ts phenotype by replica plating cells on YPD plates at both 23 and 37°C. Three colonies showed ts growth at 37°C, but grew well at 23°C. The pUN100−nic96 plasmids were recovered from these strains and the *XbaI−NdeI* DNA fragments sequenced. Two of them, named *nic96-1* and *nic96-2*, had the following mutations: P332 → L and L260 → Pro in *nic96-1* and W334 → R in *nic96-2*. Both recovered plasmids pUN100−nic96-1 and pUN100−nic96-2 were re-transformed in the NIC96 shuffle strain to confirm the plasmid-linked ts phenotype.

To construct the *GAL10::ProtA−NIC96* fusion gene, a *SphI−NheI* fragment was isolated from pBluescript−ProtA−NIC96 (Grandi *et al.*, 1993) containing the two ProtA-derived IgG binding sequences and the first 43 amino acids of Nic96p; this fragment was fused to the *URA3-GAL10* DNA isolated as an *EcoRI−SphI* fragment; finally 140 nucleotides derived from the 5′ non-coding sequence of the *NIC96* gene were placed 5′ adjacent to the *URA3* gene. To generate a suboptimal ATG start codon, the *SphI* linker GGCATGCC (New England Biolabs, Schwalbach/Taunus, Germany) was inserted at the *SphI* site found between the *NOP1* promoter and the ProtA sequence. This linear construct (5′ non-coding nic96−URA3−GAL10::ProtA−NIC96-3′) was used to replace the *NIC96* gene in the RS453 diploid strain by homologous recombination. URA^+ transformants were checked for the galactose-dependent expression of the ProtA−Nic96p fusion protein on Western blots, as described in Grandi *et al.* (1993). After tetrad analysis of such a correct integrant, GAL10::NIC96 haploid progeny were recovered. Repression of transcription of the fusion gene and the subsequent growth phenotype was measured by growing the *GAL::nic96* strain in glucose- or galactose-containing medium (YPD and YPGal).

Immunoprecipitation and indirect immunofluorescence

Immunoprecipitation experiments were performed as described in Bergès *et al.* (1994) with the following modifications. The lysis buffer used was 2% Triton X-100, 20 mM NaCl, 20 mM Tris−HCl pH 8, 5 mM $MgCl_2$ and 0.05% SDS and a protease inhibitor cocktail. The antibodies used were affinity-purified anti-Nic96 peptide antibodies, anti-Nsp1 immune serum (EC10-2) (Hurt, 1988), anti-GLFG peptide antibodies, anti-Nup57 peptide immune serum and rabbit anti-chicken IgG (Medac, Hamburg, Germany). All the strains used for the immunoprecipitation experiments were grown in YPD liquid medium, with the exception of the strains carrying the ProtA−Nic96 constructs in which selective SD-Leu medium was used. Strains were grown at 23°C prior to immunoprecipitation, except the *nup49-313* mutant strain that was grown at 30°C. Indirect immunofluorescence experiments to analyse protein import and mRNA export phenotypes were performed as described (Doye *et al.*, 1994).

Miscellaneous

DNA manipulations (restriction analysis, end-filling reactions, ligations, PCR amplifications, etc.) were performed essentially according to Maniatis *et al.* (1982). Isolation of total yeast DNA and Southern analysis were performed essentially as described in Sherman (1990).

GenBank accession number

The gene accession number for the *NUP57* gene is X81155.

Acknowledgements

We would like to thank Dr M.Hall (Basel/Switzerland) for providing plasmid YEp13::Matα2−lacZ. We gratefully acknowledge the critical reading of this manuscript by Spyros Georgatos, Catherine Dargemont and various members of the laboratory. N.S. was the recipient of a Boehringer Fellowship and E.C.H of grants from the Deutsche Forschungsgemeinschaft.

References

Akey,C.W. (1989) *J. Cell Biol.*, **109**, 955–970.
Akey,C.W. (1990) *Biophys. J.*, **58**, 341–355.
Akey,C.W. (1992) *Curr. Opin. Struct. Biol.*, **2**, 258–263.
Akey,C.W. and Radermacher,M. (1993) *J. Cell Biol.*, **122**, 1–19.
Belanger,K.D., Kenna,M.A., Wei,S. and Davis,L.I. (1994) *J. Cell Biol.*, **126**, 619–630.
Bergès,T., Petfalski,E., Tollervey,D. and Hurt,E.C. (1994) *EMBO J.*, **13**, 3136–3148.
Bonner,W.M. (1975) *J. Cell Biol.*, **64**, 421–430.
Buss,F., Kent,H., Stewart,M., Bailer,S.M. and Hanover,J.A. (1994) *J. Cell Sci.*, **107**, 631–638.
Carmo-Fonseca,M., Kern,H. and Hurt,E.C. (1991) *Eur. J. Cell Biol.*, **55**, 17–30.
Cordes,V., Waizenegger,I. and Krohne,G. (1991) *Eur. J. Cell Biol.*, **55**, 31–47.
Cordes,V.C., Reidenbach,S., Köhler,A., Stuurman,N., van Driel,R. and Franke,W.W. (1993) *J. Cell Biol.*, **123**, 1333–1344.
Dabauvalle,M.C., Benavente,R. and Chaly,N. (1988) *Chromosoma*, **97**, 193–197.
Dabauvalle,M.-C., Loos,K. and Scheer,U. (1990) *Chromosoma*, **100**, 56–66.
Davis,L.I. and Fink,G.R. (1990) *Cell*, **61**, 965–978.
Doye,V., Wepf,R. and Hurt,E.C. (1994) *EMBO J.*, **13**, 6062–6075.
Dwyer,N. and Blobel,G. (1976) *J. Cell Biol.*, **70**, 581–591.
Elledge,S.J. and Davis,R.W. (1988) *Gene*, **70**, 303–312.
Fabre,E. and Hurt,E.C. (1994) *Curr. Opin. Cell Biol.*, **6**, 335–342.
Fabre,E., Boelens,W.C, Wimmer,C., Mattaj,I.W and Hurt,E.C (1994) *Cell*, **78**, 275–289.
Featherstone,C., Darby,M.K. and Gerace,L. (1988) *J. Cell Biol.*, **107**, 1289–1297.
Feldherr,C.M., Kallenbach,E. and Schultz,N. (1984) *J. Cell Biol.*, **99**, 2216–2222.
Finlay,D.R. and Forbes,D.J. (1990) *Cell*, **60**, 17–29.
Finlay,D.R., Meier,E., Bradley,P., Horecka,J. and Forbes,D.J. (1991) *J. Cell Biol.*, **114**, 169–183.
Forbes,D.J. (1992) *Annu. Rev. Cell Biol.*, **8**, 495–527.
Gerace,L., Ottaviano,Y. and Kondor-Koch,C. (1982) *J. Cell Biol.*, **95**, 826–837.
Goldberg,M.W. and Allen,T.D. (1992) *J. Cell Biol.*, **119**, 1429–1440.
Grandi,P., Doye,V. and Hurt,E.C. (1993) *EMBO J.*, **12**, 3061–3071.
Greber,U.F., Senior,A. and Gerace,L. (1990) *EMBO J.*, **9**, 1495–1502.
Hallberg,E., Wozniak,R.W. and Blobel,G. (1993) *J. Cell Biol.*, **122**, 513–521.
Hinshaw,J.E., Carragher,B.O. and Milligan,R.A. (1992) *Cell*, **69**, 1133–1141.
Hurt,E.C. (1988) *EMBO J.*, **7**, 4323–4334.
Hurt,E.C. (1990) *J. Cell Biol.*, **111**, 2829–2837.
Jarnik,M. and Aebi,U. (1991) *J. Struct. Biol.*, **107**, 291–308.
Kita,K., Omata,S. and Horigome,T. (1993) *J. Biochem. (Tokyo)*, **113**, 377–382.
Kranz,J.E. and Holm,C. (1990) *Proc. Natl Acad. Sci. USA*, **87**, 6629–6633.
Loeb,J.D.J., Davis,L.I. and Fink,G.R. (1993) *Mol. Biol. Cell.*, **4**, 209–222.
Lupas,A., Van Dyke,M. and Stock,J. (1991) *Science*, **252**, 1162–1164.
Maniatis,T., Fritsch,E.T. and Sambrook,J. (1982) *Molecular Cloning: A Laboratory Manual.* Cold Spring Harbor Laboratory Press, Cold Spring Harbor, NY.
McKeon,F.D., Kirschner,M. and Caput,D. (1986) *Nature*, **319**, 463–468.
Morrison,H.G. and Desrosiers,R.C. (1993) *BioTechniques*, **14**, 454–457.
Mutvei,A., Dihlmann,S., Herth,W. and Hurt,E.C. (1992) *Eur. J. Cell Biol.*, **59**, 280–295.
Nehrbass,U., Kern,H., Mutvei,A., Horstmann,H., Marshallsay,B. and Hurt,E.C. (1990) *Cell*, **61**, 979–989.
Nehrbass,U., Fabre,E., Dihlmann,S., Herth,W. and Hurt,E.C. (1993) *Eur. J. Cell Biol.*, **62**, 1–12.
Panté,N. and Aebi,U. (1993) *J. Cell Biol.*, **122**, 977–984.
Panté,N. and Aebi,U. (1994) *Curr. Opin. Struct. Biol.*, **4**, 187–196.
Panté,N., Bastos,R., McMorrow,I., Burke,B. and Aebi,U. (1994) *J. Cell Biol.*, **126**, 603–617.
Reichelt,R., Holzenburg,E.L., Buhle,E.L., Jarnik,M., Engel,A. and Aebi,U. (1990) *J. Cell Biol.*, **110**, 883–894.
Richardson,W.D., Mills,A.D., Dilworth,S.M., Laskey,R.A. and Dingwall,C. (1988) *Cell*, **52**, 655–664.
Ris,H. (1989) *Inst. Phys. Conf. Ser.*, **98**, 657–662.
Rout,M.P. and Blobel,G. (1993) *J. Cell Biol.*, **123**, 771–783.

Rout,M.P. and Wente,S.R. (1994) *Trends Cell Biol.*, **4**, 357–365.
Sanger,F., Nicklen,S. and Coulson,A.R. (1977) *Proc. Natl Acad. Sci. USA*, **74**, 5466–5467.
Schlenstedt,G., Hurt,E.C., Doye,V. and Silver,P. (1993) *J. Cell Biol.*, **123**, 785–798.
Sherman,F. (1990) *Methods Enzymol.*, **194**, 3–20.
Sikorski,R.S. and Hieter,R. (1989) *Genetics*, **122**, 19–27.
Simonds,W.F., Manji,H.K., Garritsen,A. and Lupas,A.N. (1993) *Trends Biochem. Sci.*, **18**, 315–317.
Snow,C.M., Senior,A. and Gerace,L. (1987) *J. Cell Biol.*, **104**, 1143–1156.
Steinert,P.M. and Roop,D.R. (1988) *Annu. Rev. Biochem.*, **57**, 593–625.
Studier,F.W., Rosemberg,H.A., Dunn,J.J. and Dubendorff,J.W. (1990) *Methods Enzymol.*, **185**, 62–89.
Sukegawa,J. and Blobel,G. (1993) *Cell*, **72**, 29–38.
Unwin,P.N. and Milligan,R.A. (1982) *J. Cell Biol.*, **93**, 63–75.
Wente,S.R., Rout,M.P. and Blobel,G. (1992) *J. Cell Biol.*, **119**, 705–723.
Wilken,N., Kossner,U., Senécal,J.-L., Scheer,U. and Dabauvalle,M.-C. (1993) *J. Cell Biol.*, **123**, 1345–1354.
Wimmer,C., Doye,V., Grandi,P., Nehrbass,U. and Hurt,E. (1992) *EMBO J.*, **11**, 5051–5061.
Wimmer,C., Doye,V., Nehrbass,U., Schlaich,N. and Hurt,E.C. (1993) In Brown,A.J.P., Tuite,M.F. and McCarthy,J.E.G. (eds), *Protein Synthesis and Targeting in Yeast.* Springer-Verlag, Berlin, pp. 269–281.
Wozniak,R.W. and Blobel,G. (1992) *J. Cell Biol.*, **119**, 1441–1449.
Wozniak,R.K., Bartnik,E. and Blobel,G. (1989) *J. Cell Biol.*, **108**, 2083–2092.
Wozniak,R.W., Blobel,G. and Rout,M.P. (1994) *J. Cell Biol.*, **125**, 31–42.

Received on September 9, 1994; revised on October 18, 1994